

Kinetics studies of nano-structured iron catalyst in Fischer-Tropsch synthesis

Ali Nakhaei Pour^{1,2*}, Mohammad Reza Housaindokht¹,
Sayyed Faramarz Tayyari¹, Jamshid Zarkesh²

1. Department of Chemistry, Ferdowsi university of Mashhad, P. O. Box: 91775-1436, Mashhad, Iran;
2. Research Institute of Petroleum Industry of National Iranian Oil Company, P.O.Box: 14665-137, Tehran, Iran
[Manuscript received October 22, 2009; revised December 10, 2009]

Abstract

Kinetic parameters of nano-structured iron catalyst in Fischer-Tropsch synthesis (FTS) were studied in a wide range of synthesis gas conversions and compared with conventional catalyst. The conventional Fe/Cu/La catalyst was prepared by co-precipitation of Fe and Cu nitrates in aqueous media and Fe/Cu/La nanostructure catalyst was prepared by co-precipitation in a water-in-oil micro-emulsion. Nano-structured iron catalyst shows higher FTS activity. Kinetic results indicated that in FTS rate expression, the rate constant (k) increased and adsorption parameter (b) decreased by decreasing the catalyst particle size from conventional to nano-structured. Since increasing in the rate constant and decreasing in the adsorption parameter affected the FTS rate in parallel direction, the particle size of catalyst showed complicated effects on kinetic parameters of FTS reaction.

Key words

Fischer-Tropsch synthesis; iron-based catalyst; kinetics parameters

1. Introduction

The Fischer-Tropsch synthesis (FTS) is an interesting and promising pathway for the conversion of natural gas to transportation fuels [1–3]. Iron-based catalyst systems have remained a preferred choice in commercial FTS plants due to its low cost and tendency to yield high amounts of olefins in hydrocarbon distribution [4–9]. Recent studies showed nano-sized iron particles were essential to achieve high FTS activity. Some authors prepared supported iron-based Fischer-Tropsch catalysts with microemulsion method, and reported high activity and selectivity to oxygenates [10–14]. A microemulsion is optically transparent and has thermodynamically stable dispersion of water phase into an organic phase stabilized by a surfactant [15].

The kinetics of the FTS has been studied extensively to describe the reaction rate using a power law rate equation or an equation based on certain mechanistic assumptions. Recent reviews of rate equations for iron catalysts are given by Vannice [16], Huff and Satterfield [17], Zimmerman and Bukur [18], and Van der Laan and Beenackers [19]. As reported in literatures, the FTS reaction rate for iron catalysts commonly increases with H_2 partial pressure and decreases with water

partial pressure [16–19]. The mechanistic kinetic rate expressions for iron catalysts are based on the formation of the monomer species as the rate-determining step in the consumption of synthesis gas. Several theories for the formation of the monomer species were postulated in literatures [16–19]. Literature reviews indicate no reports on the effects of the catalyst particle size on the kinetic parameters of the FTS reaction in detail.

In the present work, the effects of iron particle size on kinetic parameters of FTS reaction by Fe/Cu/La catalyst have been determined. An attempt was made to discern the reasons for changes in catalyst activity and kinetic parameters with increasing of catalyst particle size.

2. Experimental

2.1. Catalyst preparation

Fe/Cu/La conventional catalyst was prepared by co-precipitation of Fe and Cu nitrates at a constant pH to form porous Fe-Cu oxyhydroxide powders. Catalyst precursor was promoted by impregnation with $La(NO_3)_3$ solution and treatment in air as described previously [4–6].

* Corresponding author. Tel/Fax: +98-21-44739716; E-mail: nakhaeipoura@ripi.ir and nakhaeipoura@yahoo.com

The Fe/Cu/La nano-catalyst precursors were prepared by co-precipitation in a water-in-oil microemulsion as described previously [10,11]. The promoted catalysts were dried at 383 K for 16 h and calcined at 773 K for 3 h in air. The catalyst compositions were designated in terms of the atomic ratios as: 100Fe/5.64Cu/2La and labeled as conv. and nano. catalysts. Based on previous results, the particle size of the conv. and nano. catalysts was determined to be 0.5 μm and 20 nm, respectively [10,11].

2.2. Catalytic performance

Steady-state FTS reaction rates and selectivities were measured in a continuous spinning basket reactor (stainless steel, $H = 0.122$ m, $D_o = 0.052$ m, $D_i = 0.046$ m) with temperature controllers (WEST series 3800). A J-type movable thermocouple made it possible to monitor the bed temperature axially, which was within 0.5 K of the average bed temperature. The reactor system also included a 50 cm³ stainless steel cold trap at ambient temperature located before the gas chromatograph sampling valve. Non-condensable gases were passed through sampling valve into an online gas chromatograph continuously then vented through a soap-film bubble meter. Separate Brooks 5850 (Brooks Instrument, USA) mass flow controllers were used to add H₂ and CO at the desired rate to admixing vessel that was preceded by a palladium trap and a molecular sieve trap to remove metal carbonyls and water before entering to the reactor. A compact pressure controller was used to control the pressure. The flow rate of tail gas is measured by a wet test gas meter.

Blank experiments show that the spinning basket reactor charged with inert silica sand without the catalyst has no conversion of syngas. The fresh catalyst is crushed and sieved to particles with the diameter of 0.25–0.36 mm (40–60 ASTM mesh). The catalyst loaded is 2.5 g and diluted by 30 cm³ inert silica sand with the same mesh size range. The catalyst samples were activated by a 5% (v/v) H₂/N₂ gas mixture with space velocity of 15.1 nl·h⁻¹·g_{Fe}⁻¹ at 0.1 MPa and 1800 rpm. The reactor temperature increased to 673 K with a heating rate of 5 K/min, was maintained for 1 h at this temperature, and then was reduced to 543 K. The activation is followed by the synthesis gas stream with H₂/CO = 1 and space velocity of 3.07 nl·h⁻¹·g_{Fe}⁻¹ for 24 h in 0.1 MPa and 543 K before the actual reaction temperature and pressure were set. After catalyst reduction, synthesis gas was fed to the reactor under conditions of 563 K, 1.7 MPa, H₂/CO in feed = 1 and a space velocity of 10.4 nl·h⁻¹·g_{Fe}⁻¹. A stabilization period of 15 h is conducted under the reaction conditions, and then the kinetics measurement is carried out. After the process conditions are changed, at least 12 h is used for the system stabilization before a new mass balance period. After reaching steady activity and selectivity, the kinetics of the Fischer-Tropsch synthesis was measured.

The external mass transfer limitation is investigated by comparing the CO conversions under different stirring speeds of the reactor. Apparently the stirring speed needed to elimi-

nate the external mass transfer limitation, which correspondingly increases with the increase of the reaction temperature. This is due to the fact that, the relative rate of external mass transfer versus the reaction rate decreases with the increase of temperature. Therefore, the corresponding stirring speed should ensure that the experimental data measured are in the kinetically limited regime. In our experiments, all the experiments were carried out at 1800 rpm which was safe to eliminate the external mass transfer limitations for all kinetic conditions. Our extensive experimental results proved that the particle diameter used in this experiment was safe for negligible intra-particle diffusion limitations. The kinetics parameters optimization later in this paper also indicates that the experimental results are free from the external and internal mass transfer limitations and in the kinetically limited regime.

For kinetic studies, a stabilization period of more than 500 h was used to ensure the stability of the catalytic phases. During the entire runs, the reactor temperature varied between 543 and 593 K, the pressure was 1.7 MPa, and the space velocity of the synthesis gas varied between 3.5 and 28.7 nl·h⁻¹·g_{Fe}⁻¹. The H₂/CO ratio of the feed kept constant in all the space velocities. Conversion of carbon monoxide and hydrogen, and the formation of various products were measured with a period of 24 h at each space velocity. Periodically during the run, the catalyst activity was measured at preset "standard" condition (a space velocity of 10.4 nl·h⁻¹·g_{Fe}⁻¹) to check the catalyst deactivation. The water partial pressure was determined by collecting the water in the trap, separating it from the oil, and weighing it. The weight of water was converted to partial pressure in the reactor based upon the ideal gas law.

The products were analyzed by means of three-dimensional gas chromatograph, a Shimadzu 4C gas chromatograph equipped with two subsequently connected packed columns: Porapak Q and Molecular Sieve 5A, and a thermal conductivity detector (TCD) with Ar as carrier gas for hydrogen analysis. A Varian CP 3800 with a Chromosorb column and a thermal conductivity detector (TCD) was used to analyse CO, CO₂, CH₄, and other non-condensable gases. A Varian CP 3800 with a Petrocol™ DH100 fused silica capillary column and a flame ionization detector (FID) was used to analyse organic liquid products so that a complete product distribution could be provided.

3. Results and discussion

Huff and Satterfield [17] proposed an FTS rate equation with water inhibition on a fused iron catalyst, based on carbide theory as well as the enol/carbide theory, which has identical mathematics as shown below:

$$-r_{\text{CO}+\text{H}_2} = \frac{kP_{\text{CO}}P_{\text{H}_2}^2}{P_{\text{CO}}P_{\text{H}_2} + bP_{\text{H}_2\text{O}}} \quad (1)$$

Based on this FTS rate expression, changes in catalyst FTS activity may be due to changes in: (i) rate constant (k), (ii) adsorption parameter (b), and (iii) partial pressure of water. The reaction rate expression given in Eq. (1) is linearized

by rearrangement as:

$$\frac{P_{H_2}}{-r_{CO+H_2}} = \frac{1}{k} + \frac{b}{k} \frac{P_{H_2}O}{P_{CO}P_{H_2}} \quad (2)$$

Hence a plot of $P_{H_2}/-r_{CO+H_2}$ versus $P_{H_2}O/P_{CO}P_{H_2}$ should give a straight line with intercept of $1/k$ and slope of b/k . In order to measure k and b in FTS rate expression (Eq. (2)) for conv. and nano catalysts, the data obtained from catalyst activity tests at various conversions are plotted in Figure 1. As shown in this Figure, the results for carbon monoxide conversions of less than 60% lie on a straight line but the results for higher carbon monoxide conversions deviate substantially

for both catalysts because the FTS reaction highly depends on the hydrogen formed by the WGS as the carbon monoxide conversion increases. Thus, the overall FTS reaction rate is highly affected by the rate/extent of the WGS reaction at high FTS conversions. The FTS reaction rate is unaffected by the WGS reaction only at lower conversions [20]. In order to estimate the FTS reaction rate, regression lines in Figures 2 to 3, were drawn for the data at carbon monoxide conversions below 60%. Obtained data from these regression lines corresponded only to the FTS reaction. The intercept and slope of the regression lines were used to calculate the rate constant (k) and the adsorption parameter (b) for conv. and nano. catalysts.

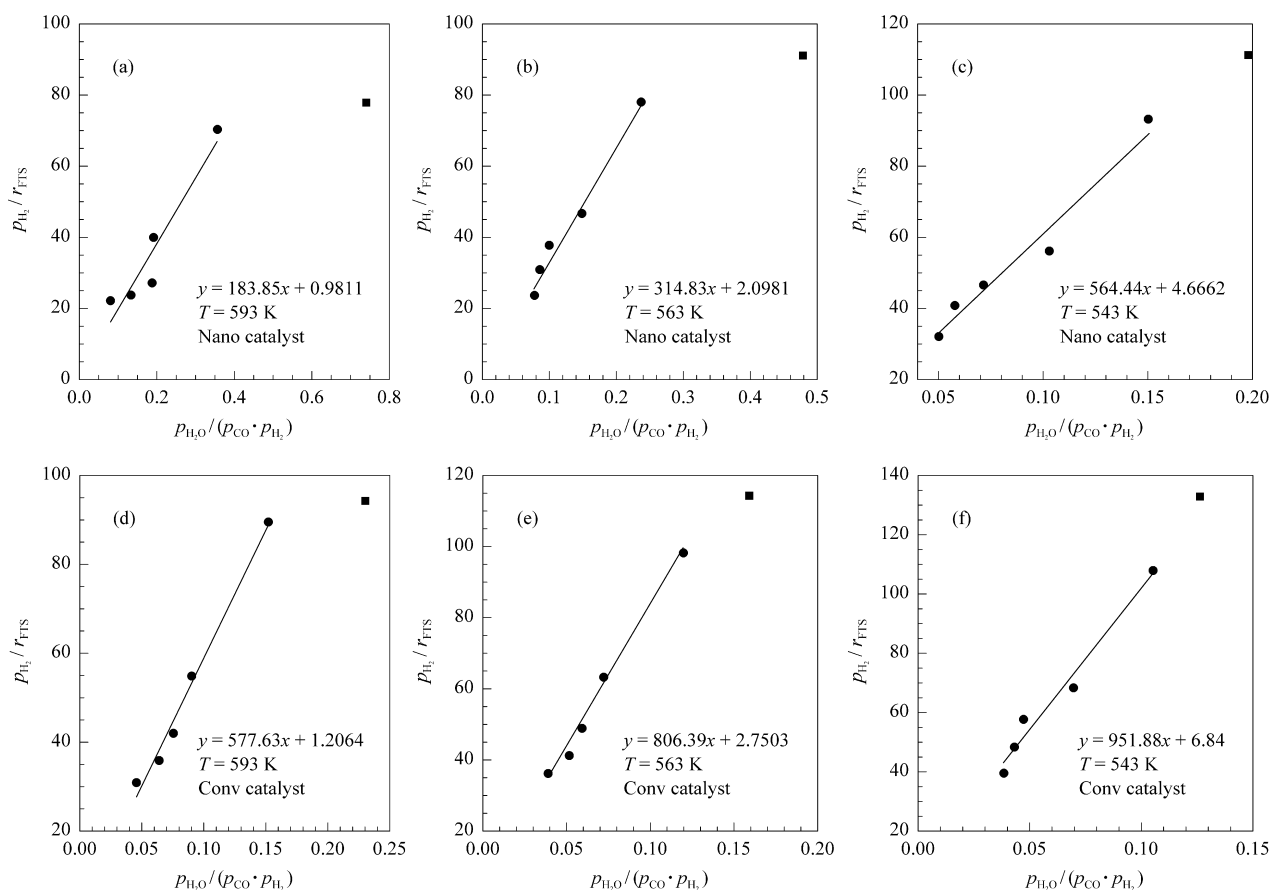


Figure 1. Plots of the linearised form of rate equation according to Huff and Satterfield

The calculated rate constant (k) and the adsorption parameter (b) at various temperatures for conv. and nano. catalysts are listed in Table 1. Table 1 depicted that by decreasing the catalyst particle size from conv. to nano, catalysts, the rate

constant (k) for FTS reaction was increased and the adsorption parameter (b) was decreased. These results showed that the FTS rate was increased with decreasing the catalyst particle size.

Table 1. Calculated kinetic parameters of catalysts

Catalyst	Particle size	$k/\text{mol}/(\text{g}_{\text{cat}} \cdot \text{h} \cdot \text{bar})$			b/bar			E_a/kJ	$\Delta H/\text{kJ}$
		593 K	563 K	543 K	593 K	563 K	543 K		
Conv.	0.5 μm	0.83	0.36	0.15	474	293	139	92	64
Nano.	20 nm	1.02	0.48	0.22	187	150	121	83	23

The dependency of the reaction rate constant on temperature is described by the Arrhenius equation. The activation energy is determined using the Arrhenius equation that directly introduced into the kinetic parameters:

$$k = k_{\infty} \exp\left(\frac{-E_a}{RT}\right) \quad (3)$$

Hence, a plot of $\ln(k)$ versus $1/T$ should give a straight line with slope of $-E_a/R$. The logarithm of the rate constant (k) is plotted in Figure 2 as a function of reciprocal temperature for catalysts. From the slope of the curves in Figure 2, the activation energies are determined to be 92 and 83 kJ/mol for conv. and nano catalysts, respectively. It means that by decreasing the catalyst particle size, the activation energy of FTS reaction decreased and as a result, FTS reaction rate increased.

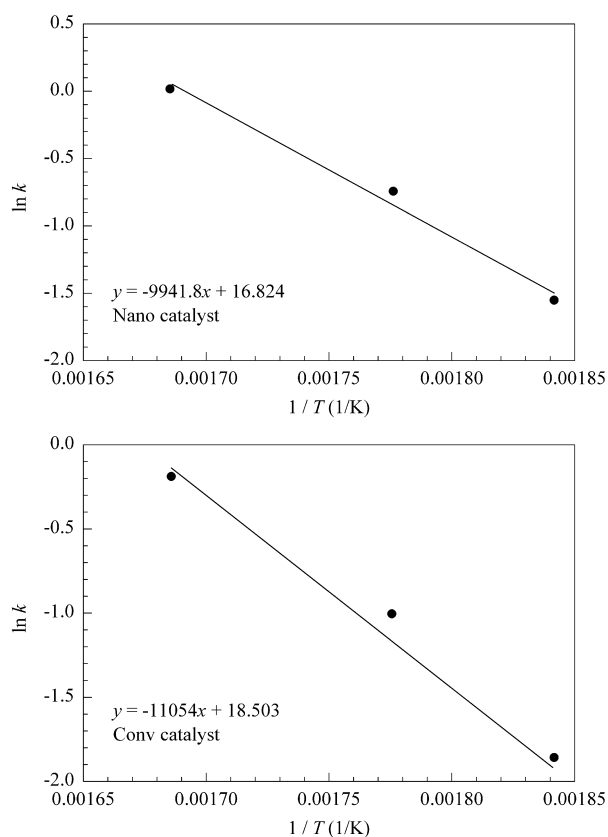


Figure 2. Arrhenius plot of rate constant (k)

The adsorption parameter (b) in Huff and Satterfield kinetic model [17] is equal to K_{H_2O}/K_{CO} , where K_{H_2O} and K_{CO} are adsorption equilibrium constants for water and carbon monoxide, respectively. Table 1 depicted that by decreasing the catalyst particle size, the adsorption parameter b was decreased. Decreasing in the adsorption parameter (b) can be due to decreasing the adsorption equilibrium constant for water (K_{H_2O}) and/or an increase in the adsorption equilibrium constant for carbon monoxide (K_{CO}). Previous studies have shown that the lower particle size caused an increase in the adsorption equilibrium constant for carbon monoxide [10,11].

Adsorption enthalpy $\Delta H_{ads,b}$ can be determined with adsorption parameter b via:

$$b = b_{\infty} \exp\left(\frac{-\Delta H_{ad}}{RT}\right) \quad (4)$$

The logarithm of the parameter b is plotted in Figure 3 as a function of reciprocal temperature for catalysts. From the slope of the curves in Figure 3, the heats of adsorption for b are determined to be 64 and 23 kJ/mol for conv. and nano. catalysts, respectively.

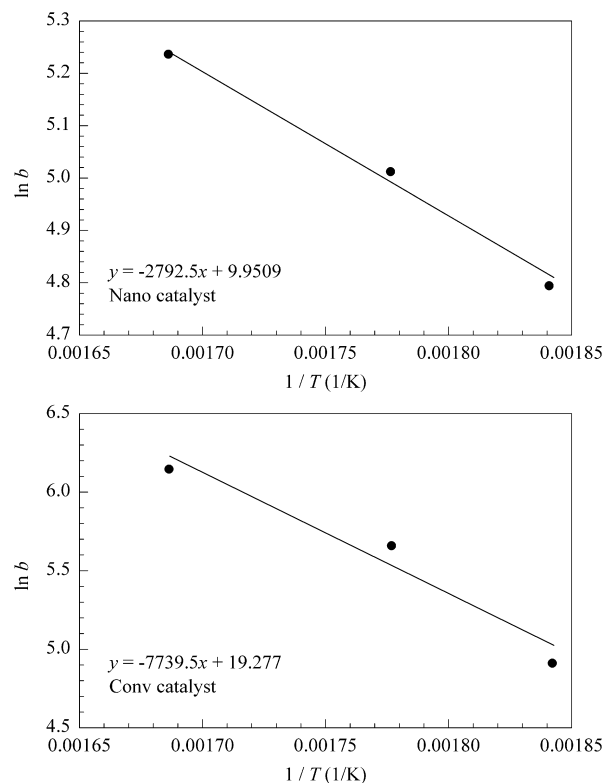


Figure 3. Adsorption parameter (b) as a function of $1/T$

4. Conclusions

Particle size of precipitated iron catalyst has shown significant influences on rate constant (k) and adsorption parameter (b) in kinetic models proposed by Huff and Satterfield [17]. Kinetic results indicated that in FTS rate expression, the rate constant (k) increased by decreasing the catalyst particle size from conventional to nano-structured, which means that the FTS reaction rate increased by decreasing the catalyst particle size. In addition, the adsorption parameter (b) was decreased by decreasing the catalyst particle size, because of decreasing in the adsorption equilibrium constant for water and/or an increase in the adsorption equilibrium constant for carbon monoxide. Since that, both increasing in the rate constant and decreasing in the adsorption parameter enhanced the FTS rate, the particle size of catalyst showed complicated effects on kinetic parameters of FTS reaction.

References

- [1] Anderson R B. The Fischer-Tropsch Synthesis. Orlando, FL: Academic Press, 1984
- [2] Bartholomew C H. *Stud Surf Sci Catal*, 1991, 64: 158
- [3] Dry M E. In: Anderson J R, Bourdard M ed. Catalysis: Science and Technology, Vol II. New York: Springer-Verlag, 1981. Chapter 4
- [4] Pour A N, Shahri S M K, Zamani Y, Irani M, Tehrani S. *J Natur Gas Chem*, 2008, 17(3): 242
- [5] Pour A N, Zamani Y, Tavasoli A, Kamali Shahri S M, Taheri S A. *Fuel*, 2008, 87(10-11): 2004
- [6] Pour A N, Shahri S M K, Bozorgzadeh H R, Zamani Y, Tavasoli A, Marvast M A. *Appl Catal A*, 2008, 348(2): 201
- [7] Li S, Li A, Krishnamoorthy S, Iglesia E. *Catal Lett*, 2001, 77(4): 197
- [8] Yang J, Sun Y, Tang Y, Liu Y, Wang H, Tian L, Wang H, Zhang Z, Xiang H, Li Y W. *J Mol Catal A*, 2006, 245(1-2): 26
- [9] Tao Z, Yang Y, Zhang C, Li T, Wang J, Wan H, Xiang H, Li Y. *Catal Commun*, 2006, 7(12): 1061
- [10] Pour A N, Taghipoor S, Shekarriz M, Shahri S M K, Zamani Y. *J Nanosci Nanotechno*, 2009, 9(7): 4425
- [11] Pour A N, Housaindokht M R, Tayyari S F, Zarkesh J. *J Natur Gas Chem*, 2010, 19: 284
- [12] Sarkar A, Seth D, Dozier A K, Neathery J K, Hamdeh H H, Davis B H. *Catal Lett*, 2007, 117(1-2): 1
- [13] Herranz T, Rojas S, Pérez-Alonso F J, Ojeda M, Terreros P, Fierro J L G. *Appl Catal A*, 2006, 311: 66
- [14] Eriksson S, Nylén U, Rojas S, Boutonnet M. *Appl Catal A*, 2004, 265(2): 207
- [15] Schwuger M J, Stickdorn K, Schomaecker R. *Chem Rev*, 1995, 95(4): 849
- [16] Vannice M A. *Catal Rev-Sci Eng*, 1976, 14(2): 153
- [17] Huff G A, Satterfield C N. *Ind Eng Chem Process Des Dev*, 1984, 23(4): 696
- [18] Zimmerman W H, Bukur D B. *Can J Chem Eng*, 1990, 68(2): 292
- [19] Van der Laan G P, Beenackers A A C M. *Catal Rev-Sci Eng*, 1999, 41(3-4): 255
- [20] Raje A P, O'Brien R J, Davis B H. *J Catal*, 1998, 180(1): 36